THE ASTROPHYSICAL JOURNAL, 227:391–397, 1979 January 15

PLANETARY NEBULAE IN LOCAL GROUP GALAXIES. VII. SPECTROPHOTOMETRY AND FILTER PHOTOMETRY OF M32–1

DAVID C. JENNER,* HOLLAND C. FORD,* AND GEORGE H. JACOBY
Department of Astronomy, University of California, Los Angeles
Received 1978 April 26; accepted 1978 August 1

ABSTRACT

M32–1 is a relatively bright planetary nebula in the small elliptical galaxy M32. Seven spectrophotometric scans of the nebula were obtained at Lick Observatory and at Kitt Peak National Observatory. The resulting emission-line flux ratios provide qualitative and quantitative indications of chemical abundances in the nebula. That the nitrogen-to-hydrogen emission-line ratio is large even though the nebula is of intermediate to moderately high excitation suggests a possible enrichment of nitrogen. The number abundance of helium to hydrogen is 0.10 ± 0.05. Filter photometry obtained at Lick Observatory shows that the luminosity in [O III] λ5007 of M32–1 is comparable to the luminosity of the brightest planetary nebulae in the Large Magellanic Cloud and in M31 and that the mass of ionized gas is approximately 0.09 $M_{\odot}$ for an assumed value of $n_e = 10^4$ cm^{-3}.

Subject headings: galaxies: individual — nebulae: abundances — nebulae: individual — nebulae: planetary — spectrophotometry

I. INTRODUCTION

A primary objective of the study of planetary nebulae in Local Group galaxies is to obtain photoelectric spectrophotometry of nebular emission lines. The observed emission-line fluxes provide qualitative comparisons of physical conditions among nebulae, provide a means for studying interstellar extinction external to the Milky Way galaxy, and in some cases provide quantitative measurements of chemical abundances. Careful spectrophotometric observations also provide nebular radial velocities. The radial velocities indicate the systemic velocity of the parent galaxy and allow the investigation of the velocity field within the galaxy. This paper concentrates on the presentation of spectrophotometric and filter photometric observations of a relatively bright nebula in the small elliptical galaxy M32 and on the resulting ionic abundances and nebular mass.

Paper I (Ford, Jenner, and Epps 1973) and Paper II (Ford and Jenner 1975) of this series present identifications of planetary nebulae in M32. Both of those papers denote the nebulae studied in this paper as nebula number 1 in M32 (M32–1). A description of the observations and reductions for M32–1 appears in § II; the resulting emission-line fluxes are derived in § III; and the emission-line ratios, the abundances, and the nebular mass determined for M32–1 are discussed in § IV.

II. OBSERVATIONS AND REDUCTIONS

The observations of M32–1 were made with the 3 m Shane telescope at Lick Observatory and the 4 m Mayall telescope at Kitt Peak National Observatory. In both cases similar instruments and similar observing techniques were employed. At Lick the image-tube scanner (ITS), originally called the image-dissector scanner (IDS) (Robinson and Wampler 1972, 1973), was used; at Kitt Peak the intensified image-dissector scanner (IIDS) was used. In both cases the nebula was acquired by means of accurate blind offsets from nearby reference stars (see Paper II) visible on the television acquisition systems. Small-scale variations in the detector sensitivity were corrected by observing a continuum lamp, while observations of standard stars (Stone 1974, 1977) provided a determination of the variation of system sensitivity with wavelength. Helium-neon-argon lamps were observed so that the wavelength scales could be linearized. Table 1 is a journal of observations which summarizes the characteristics of the resulting spectrophotometric scans.

a) *Lick Observations*

Our typical observing procedure at Lick is outlined in Paper IV (Ford, Jacoby, and Jenner 1977). Two 2″ × 2″ apertures were used usually in a beam-switched mode to facilitate simultaneous "object + sky" and "sky" observations for later sky subtraction. The characteristics of the scans are included in Table 1. The different spectrographs and detectors are described in detail by Osterbrock and Miller (1975) and by Phillips and Osterbrock (1975).

Figures 1, 2, and 3 contain examples of Lick scans—after they were reduced as described below. Inspection of the short, individual scans summed to produce scan 4 (Fig. 2) suggests that the emission line near λ4363 is due to poor subtraction of mercury λ4358 in city lights rather than to [O III]. Figure 3 (scan 7) is actually the sum of four separate observations made

* Visiting Astronomer, Kitt Peak National Observatory, which is operated by the Association of Universities for Research in Astronomy, Inc., under contract with the National Science Foundation.

TABLE 1

JOURNAL OF OBSERVATIONS

SCAN NO.	1	2	3	4	5	6	7
Figure No.	1	1	-	2	-	4	3
Date (UT)	1972 Nov 30	1972 Dec 2	1974 Sep 18	1974 Oct 14	1975 Sep 7	1976 Nov 19	1974 Fall
Telescope	Lick 3m	Lick 3m	Lick 3m	Lick 3m	Lick 3m	KPNO 4m	Lick 3m
Spectrograph	Old	Old	New	New	New	Gold	New
Detector	Old IDS	Old IDS	New ITS	New ITS	New ITS	IIDS	New ITS
Image Tube Sensitivity	Red	Red	Red	Red	Blue	Blue	Red
Dwell Time (minutes)	120	144	12	72	56	32	104
Grating							
Grooves/mm	600	600	600	831	600	300	1200
Blaze λ(Å)	5000	5000	5000	4400	5000	6750	5000
Order	1st	1st	1st	2nd	1st	1st	1st
Central λ(Å)	5200	5200	5800	4700	4050	5100	6560
λRange (Å)	2400	2400	2400	900	2250	3525	1200
Reciprocal Dispersion (Å/mm)	103	103	154	56	154	176	78
Resolution (Å)	8	8	8	3	8	12	4
Standard Star	Feige 15	Hiltner 600	Feige 15	HZ 15	+28° 4211 +33° 2642	Feige 34	(none)

during the fall of 1974, two of which were made in a beam-switched mode and two of which were made with a single aperture. The only reductions made on these data are the summation and the accompanying sky subtraction. Since the variation of detector sensitivity, atmospheric extinction, and nonlinearity of wavelength scale over the range of wavelengths from 6548 to 6584 Å is small, we treat the resulting data as fully reduced with little error introduced.

b) *Kitt Peak Observations*

Our typical observing procedure at Kitt Peak is outlined in Paper III (Ford and Jenner 1976). Only one of two 3″ circular apertures was used with alternation between "object + sky" and "sky" observations for later sky subtraction. The characteristics of the resulting scan (scan 6) are included in Table 1. Although the scan of M32–1 was calibrated

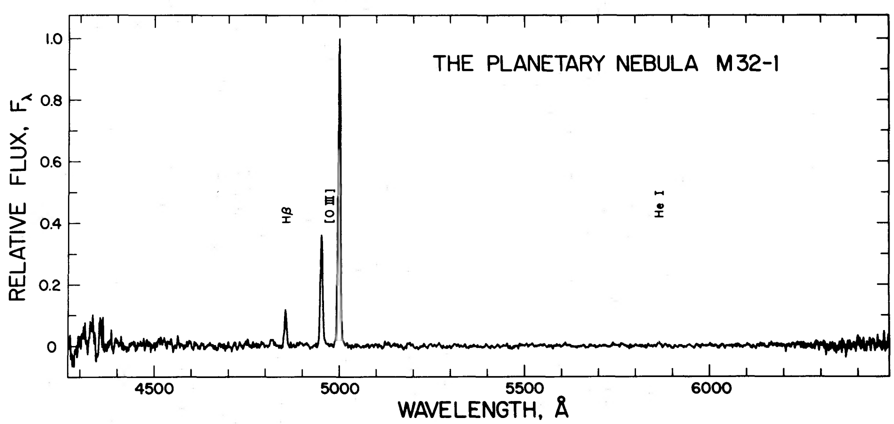

FIG. 1.—Sum of scans 1 and 2 of Table 1 made at Lick Observatory; fully reduced flux $F(\lambda)$ is plotted versus λ as described in text.

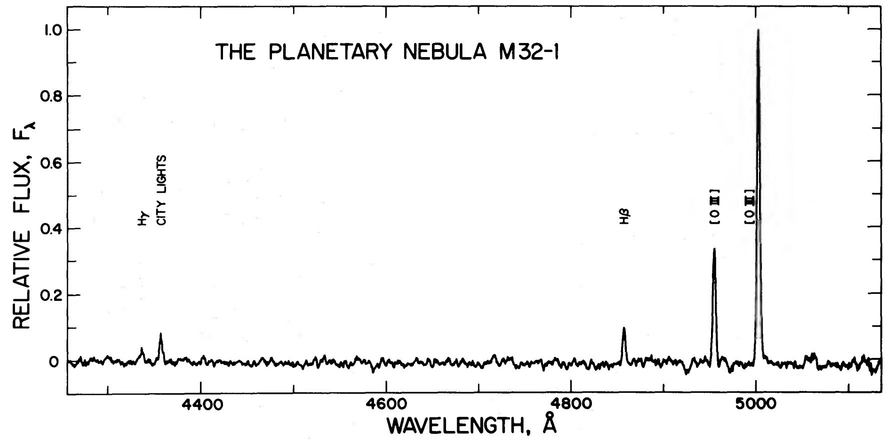

FIG. 2.—Scan 4 of Table 1 made at Lick Observatory; fully reduced flux $F(\lambda)$ is plotted versus λ as described in text

using the standard star Feige 34, confirmation of the calibration was made by also observing the small-planetary nebulae IC 5217 and IC 351 (Peimbert and Torres-Peimbert 1971; Minkowski and Aller 1956). Figure 4 shows the Kitt Peak scan—after it was reduced as described below.

c) *Spectrophotometric Reductions*

All the raw data (with the exception of the scans summed to produce scan 7) were reduced to a linear wavelength scale and a linear intensity scale using standard spectrophotometric techniques as described by Osterbrock and Miller (1975), Phillips and Osterbrock (1975), and Osterbrock (1977). Lick Observatory PDP-8 reduction programs and a comparable system developed by G. H. J. at UCLA for a PDP-11 minicomputer gave results equivalent to within a few percent of the maximum flux of a scan.

d) *Total Emission-Line Fluxes*

The observed line profile of an emission line is determined by the finite resolution of the spectrograph-detector system; that resolution varies slightly across each scan. Therefore, in order to properly measure the total emission-line flux, it is necessary to integrate under the line profile of an emission line rather than to measure just its height above the background. Furthermore, several of the scans (especially the Lick "blue" observation) have wings on the line profiles which contain a significant amount of the total flux observed. Those wings tend to be neglected when two or more lines are blended or when a line is weak compared to the noise in the background. Our measurement of areas to get total emission-line fluxes consequently uses a fitting procedure developed by C. M. Price in order to best treat blends and weak lines.

An analytic line-profile function that includes a "wing" parameter is first fitted to a strong, unblended emission line in a scan. Then an attempt is made to least-squares fit the line-profile function to the data in a scan at wavelengths where emission lines are expected. If the standard deviation of the fitted area is less than the resultant area, the area is taken as the measurement of the total emission-line flux. If the standard deviation is greater than the resultant area, the standard deviation is used as an upper limit to the observed emission-line flux. This procedure is objective, but it often produced an upper limit that exceeded a visually estimated one.

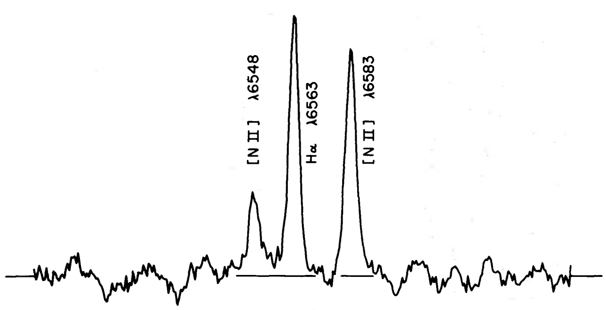

FIG. 3.—Scan 7 of Table 1 made at Lick Observatory; partially reduced data are the sum of four separate observations.

e) *Filter Photometry at λ5007*

Because of the small apertures used for the spectrophotometry, the effects of setting errors, guiding errors, seeing, and atmospheric dispersion generally produce unreliable absolute measurements of the emission-line fluxes. However, photoelectric filter photometry of M32-1 allows conversion of the relative fluxes in Table 1 to absolute units. The photometry was performed in conjunction with photometry of planetary nebulae in M31 (Paper V [Ford and Jacoby 1978]). The observed flux in [O III] λ5007 of M32-1 is 1.2×10^{-14} ergs cm^{-2} s^{-1} as determined from a total of 880 s of integration time. This value is two-thirds the observed value for M31-116, the brightest planetary nebula measured to date in M31.

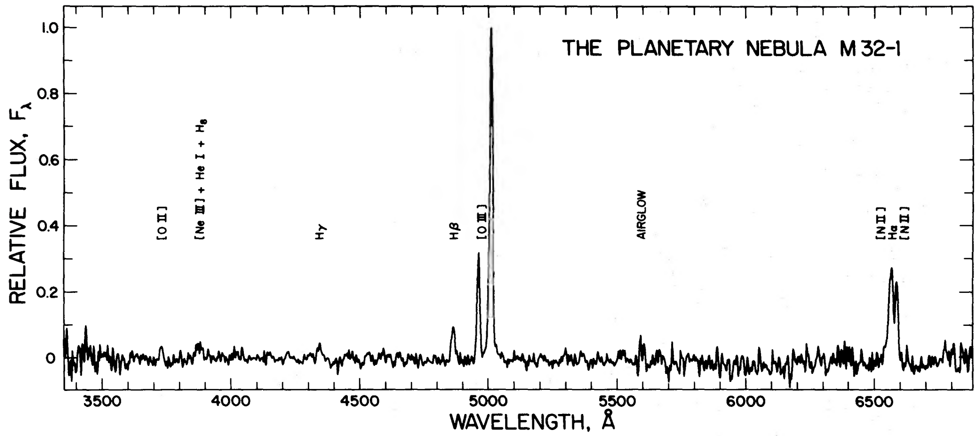

FIG. 4.—Scan 6 of Table 1 made at Kitt Peak National Observatory; fully reduced flux $F(\lambda)$ is plotted versus λ as described in text.

III. RESULTS

The results of the reductions outlined in § II are total emission-line fluxes for each of the seven scans described in Table 1. This section describes the combining of those individual scans to get average fluxes and the correcting of the average fluxes for interstellar reddening due to dust in our Galaxy.

a) Individual Scan Results

Table 2 lists for each ion and rest wavelength the total emission-line flux normalized to the flux observed

TABLE 2

M32-1 EMISSION-LINE FLUXES

SCAN NO. Ion	 λ	1	2	3	4 F(λ)/F(5007) Counts	5	6	7	Average <F(λ)/F(5007)> Std. Error	Ratio <F(λ)/F(4861)> [E(B-V)=0.11]
[OII]	3727					0.073 173	0.051 111		0.062 0.011	0.63
H I + He I + [NeIII]	3889					0.125 576	0.069 341		0.096 0.028	0.96
H I δ	4101	<0.004				0.031 122	<0.004		0.031:	0.30:
H I γ	4340	0.025 189	0.032 110		0.046 210	0.048 261	0.041 334		0.038 0.004	0.36
He II	4686	<0.001	<0.011		<0.009	<0.034	<0.028		<0.017:	<0.15:
H I β	4861	0.102 721	0.102 540	0.105 193	0.111 842	0.118 1262	0.111 923		0.110 0.003	1.00
[OIII]	4959	0.333 2490	0.360 2138	0.253 537	0.359 2405	0.303 3187	0.316 2300		0.326 0.013	2.92
[OIII]	5007	1.000 7304	1.000 6193	1.000 2094	1.000 7006	1.000 9360	1.000 8543		1.000	8.97
He I	5876	0.018 127	0.011 108	<0.024			<0.011		0.014 0.003	0.12
[NII]	6548			0.096 158			0.084 234	0.117 12832	0.116 0.004	0.94
H I α	6563			0.354 582			0.310 865	(0.326) 31734	0.326 0.021	2.64
[NII]	6584			0.288 474			0.252 703	0.311 29064	0.309 0.007	2.50
[SII]	6717			0.042 41					0.042:	0.34:
[SII]	6731			0.075 73					0.075:	0.60:

for [O III] λ5007. One exception to this normalization is scan 7, where Hα λ6563 is normalized to the average value of Hα found from scans 3 and 6. The normalized fluxes $F(\lambda)/F(5007)$ are the fractional values appearing in each of the seven columns labeled by scan number. Approximate upper limits to very weak lines are preceded by a < sign.

Just below each normalized flux is an integer "count" N for that scan and emission line. That count is an estimate of the actual number of *photons* counted for that emission line. The counts were obtained by integrating the areas under emission lines in the raw data (only sky subtraction made) to get total counts of *photoelectrons*. Then the counts of photoelectrons were divided by the known average ratio of photoelectrons per detected photon for the appropriate detector system. The ratios used were 8 and 6 for the Lick "red" and "blue" scans, respectively (M. Gaskell, private communication), and 1.2 for the Kitt Peak scan (L. Goad, private communication). These values are approximate and in fact vary slightly across a scan, but the resulting estimate of counts (photon events) is adequate for the method of averaging described below.

b) *Average Results*

Since the scans listed in Table 1 result from different observational situations, an objective method of combination of the individual results was chosen and utilized. The basic assumptions made when combining results from different scans are that the standard star observations are errorless, that the flux of the strongest line is known exactly, and that the dominant source of error of other lines is the statistical fluctuation in the counting of nebular photons. The statistical fluctuations in the counting of "sky" photons are neglected in the present case—a good assumption except for He I λ5876. In this case a consideration of Poisson statistics shows that the average flux $\langle F \rangle$ is given by

$$\langle F \rangle = \frac{\sum N_i}{\sum T_i}\,, \tag{1}$$

where each sum is made over all scans i to be included. Here N_i is the number of photons counted in the ith scan and T_i is a "generalized interval" which includes the dwell time, the telescope collection area, the sensitivity of the telescope-spectrograph-detector system, and the transparency of the Earth's atmosphere. Note that the flux for the ith scan is just

$$F_i = \frac{N_i}{T_i} \tag{2}$$

and that this is the quantity produced by the reductions outlined in §§ II*c* and II*d*.

The average flux, obtained by combining equations (1) and (2), is simply

$$\langle F \rangle = \frac{\sum T_i F_i}{\sum T_i} \tag{3a}$$

$$= \frac{\sum N_i}{\sum (N_i/F_i)}\,, \tag{3b}$$

where we know both F_i and N_i from Table 2. In this particular case, we calculate an average flux with weights equal to the generalized intervals for each scan. For a truly Poisson process the *expected* variance σ_e^2 of the average flux $\langle F \rangle$ is given by

$$\sigma_e^2 = \frac{\langle F \rangle}{\sum T_i} = \frac{\langle F \rangle}{\sum (N_i/F_i)}\,, \tag{4}$$

while the *observed* variance σ_o^2 of the average flux is given by

$$\sigma_o^2 = \frac{1}{(n-1)}(\langle F^2 \rangle - \langle F \rangle^2)\,, \tag{5}$$

where the average-squared flux is defined with weights T_i as in equation (3a) and n is the number of scans combined.

The suitability of the adopted Poisson model may be tested by performing a χ^2 test with $n - 1$ degrees of freedom, where

$$\chi^2 \approx (n-1)\frac{\sigma_o^2}{\sigma_e^2}\,. \tag{6}$$

For the data in Table 2 such a χ^2 test (with a smaller than desirable sample size, unfortunately) shows that statistical fluctuations are likely to be the dominant source of error only for emission lines of intermediate strength in the present scans. Apparently, other sources of error (such as variable atmospheric extinction) often equal or surpass statistical fluctuations in importance. Since it is difficult or impossible to model all other such sources of error easily and accurately, we proceed to use the Poisson model.

Table 2 contains the emission-line fluxes averaged as in equation (3b) in the colum labeled "Average $\langle F(\lambda)/F(5007)\rangle$." Also given in that column—directly below the average for a given emission line—is the *observed* standard error σ_o as found from equation (5). Average values for which only one determination other than approximate upper limit is available are followed by a colon. Note that the standard errors vary from 3% or 4% for a strong, unblended line to 20% or 30% for the weakest lines.

c) *Galactic Interstellar Extinction*

The final correction made to the data in Table 2 is one for selective extinction due to dust in our Galaxy. Paper VI (Ford, Jacoby, and Jenner 1978) discusses in detail the galactic extinction and possible extinction due to dust in M31. Basically, we adopt the color excess $E(B - V) = 0.11$ mag found by McClure and

Racine (1969) for late-type stars in the direction of M31. This value produces an observed Balmer decrement that is consistent, within errors, with recombination theory (Brocklehurst 1971). Note that M32 is therefore placed along the line of sight *in front of* M31 (Paper IV).

The adopted color excess and the Whitford reddening curve (Whitford 1958) produce corrected fluxes which are then renormalized so that, for Hβ, $F(4861) = 1$. The final column of Table 2 contains the final emission-line flux ratios.

When the observed flux in [O III] λ5007 is corrected for interstellar extinction (assuming $R = 3$), the resulting flux is 1.6×10^{-14} ergs s^{-1} cm^{-2}. Note that, for a correct comparison, the observed values in M31 (Paper V) should be corrected by an approximately equal factor. A comparison of M32–1, M31–116, and the brightest LMC planetaries (Webster 1969) reveals that these bright nebulae all have the same [O III] λ5007 luminosity to within a factor of 2.

IV. EMISSION-LINE RATIOS, ABUNDANCES, AND THE NEBULAR MASS

Several of the final emission-line flux ratios provide results of astrophysical interest. Since we were unable to make a direct determination of electron temperature and density, most of the line ratios provide only qualitative comparison criteria. The helium abundance is quantitatively, but inaccurately, determined. The mass of the nebular shell may be estimated if an electron density is assumed.

The Balmer decrements and their uncertainties are

$$\frac{F(\mathrm{H}\alpha)}{F(\mathrm{H}\beta)} = 2.64 \pm 0.27$$

and

$$\frac{F(\mathrm{H}\alpha)}{F(\mathrm{H}\gamma)} = 7.33 \pm 1.24\,.$$

The uncertainties are standard errors calculated by propagation of error from the values in Table 2 with assumption that the correction for interstellar reddening is known exactly. In both cases the expected Balmer decrement (Brocklehurst 1971) of a typical planetary nebulae ($n_e = 10^4$ cm^{-3}, $T_e = 10^4$ K) falls within 1 standard error of the above decrements.

Inspection of the ratios $F(5007 + 4959)/F(4861)$, $F(3727)/F(4959)$, and $F(4686)/F(4861)$ shows that M32–1 is of intermediate to moderately high excitation—Aller and Liller (1968) excitation class 5–7. The high ratio of [N II] λ6584 to Hα λ6563 is somewhat unusual for this high an excitation class. Observations of a total of 11 planetary nebulae in M32 show, however, that strong nitrogen lines are the rule rather than the exception in M32; the average ratio is 0.6, and nitrogen was undetected in only one nebula. For comparison, a total of four nebulae in NGC 147, NGC 185, and NGC 205 have comparatively weak nitrogen lines; the average ratio is less than 0.1. This suggests that there is some fundamental physical difference between the brightest planetary nebulae in M32 and the brightest in other galaxies, even though the progenitor stars in these galaxies are likely to be of the same age. Of all extragalactic planetary nebulae observed photoelectrically, M32–1 is most like L16, P7 in the LMC (Osmer 1976). Osmer finds for that nebula an overabundance of nitrogen by a factor of 2 relative to a mean of galactic planetary nebulae. However, the nitrogen line strengths are known to vary greatly and systematically within a single nebula (see, e.g., Hawley and Miller 1977) because of the variation in degree of ionization with constant nebular nitrogen abundance. The weighted-average nitrogen line strengths that we observe from the entirety of the M32 nebulae could result from such ionization effects.

Further information, including the determination of an electron temperature, is needed before a choice between the several possibilities (enhanced nitrogen abundance, temperature and/or density variations, central star differences) for the production of strong nitrogen lines may be made for M32. The simplest suggestion is that the nitrogen abundance is systematically enhanced in M32, but this matter will be investigated again in later papers as the data for all nebulae are fully reported.

The ratio of [S II] $F(6717)/F(6731)$ is very poorly determined. The observed ratio is consistent, however, with an electron density of $n_e = 10^4$ cm^{-3} for an assumed $T_e = 10^4$ K (Czyzak, Krueger, and Aller 1970).

For helium, a quantitative, although uncertain, abundance results. The observed line ratios for He I and He II are

$$\frac{F(5876)}{F(4861)} = 0.12 \pm 0.03$$

and

$$\frac{F(4686)}{F(4861)} \lesssim 0.14\,.$$

Contamination by H I and [Ne III] makes utilization of $F(3889)$ to estimate the helium abundance undesirable. The above ratios along with the expressions presented by Miller (1974) give

$$\frac{n(\mathrm{He}^+)}{n(\mathrm{H}^+)} = 0.089 \pm 0.038$$

and

$$\frac{n(\mathrm{He}^{++})}{n(\mathrm{H}^+)} \lesssim 0.012$$

for an assumed electron temperature of $10^{4\pm0.3}$ K. When the upper limit for He^{++} is adopted as both its abundance and uncertainty and when a negligible contribution by neutral helium is assumed, the number abundance of helium to hydrogen is

$$\frac{n(\mathrm{He})}{n(\mathrm{H})} = 0.10 \pm 0.05\,.$$

This value is consistent with the nominal helium abundance found for galactic and extragalactic gaseous nebulae (Peimbert 1975). Most of the estimated error results from the uncertainty in the two observed line ratios. This uncertainty prevents a precise investigation of the evolutionary enrichment of helium and metals as suggested by Peimbert.

The mass of the gas in the ionized shell can be estimated in the following way. The quantity $n_e n_+ V$—the product of the electron density, proton density, and volume producing the emission—is determined from the Hβ flux [F(Hβ)], the distance to the nebula (D), and the emission coefficient (j_β):

$$n_e n_+ V = \frac{F(\mathrm{H}\beta) 4\pi D^2}{(4\pi j_\beta / n_e n_+)}\,.$$

The extinction-corrected [O III] λ5007 flux and the Hβ to λ5007 flux ratio from § III*c* produce $F(\mathrm{H}\beta) = 1.8 \times 10^{-15}$ ergs s^{-1} cm^{-2}. We adopt $D = 660$ kpc and assume $T_e = 10^4$ K so that $4\pi j_\beta / n_e n_+ = 1.24 \times 10^{-25}$ ergs s^{-1} cm^{-3} (Osterbrock 1974). The mass of the ionized gas in the shell is given by

$$M = 1.4 m_{\mathrm{H}} n_+ V = \frac{1.4 m_{\mathrm{H}}(n_e n_+ V)}{n_e}\,,$$

where m_{H} is the proton mass and the factor 1.4 accounts for the contribution of helium to the mass. If we assume $n_e = 10^4$ cm^{-3}, then

$$M = 0.09\, M_\odot\,,$$

with an order of magnitude uncertainty. This value compares favorably with the average mass of ionized gas in an average planetary nebula in our Galaxy and the LMC (Osterbrock 1974). Unless $n_e \geq 10^5$ cm^{-3}, the nebular mass is more nearly that of a disk population planetary nebula than that of the halo population nebula M15:K648 (Peimbert 1973).

We thank the Director and Time Assignment Committee at Kitt Peak for the allocation of observing time. We also thank Dr. H. W. Epps for several discussions about statistics and Ms. K. Sedwick for carefully making the figures. Computer time was funded by a grant from the Office of Academic Computing. This research was sponsored in part by NSF grant AST 76-21312 to H. C. F.

REFERENCES

Aller, L. H., and Liller, W. 1968, in *Nebulae and Interstellar Matter*, ed. B. M. Middlehurst and L. H. Aller (Chicago: University of Chicago Press), p. 483.
Brocklehurst, M. 1971, *M.N.R.A.S.*, **153**, 471.
Czyzak, S. J., Krueger, T. K., and Aller, L. H. 1970, *Proc. Nat. Acad. Sci.*, **66**, 282.
Ford, H. C., and Jacoby, G. H. 1978, *Ap. J.*, **219**, 437 (Paper V).
Ford, H. C., Jacoby, G., and Jenner, D. C. 1977, *Ap. J.*, **213**, 18 (Paper IV).
———. 1978, *Ap. J.*, **223**, 94 (Paper VI).
Ford, H. C., and Jenner, D. C. 1975, *Ap. J.*, **202**, 365 (Paper II).
———. 1976, *Ap. J.*, **208**, 683 (Paper III).
Ford, H. C., Jenner, D. C., and Epps, H. W. 1973, *Ap. J. (Letters)*, **183**, L73 (Paper I).
Hawley, S. A., and Miller, J. S. 1977, *Ap. J.*, **212**, 94.
McClure, R. D., and Racine, R. 1969, *A.J.*, **74**, 1000.
Miller, J. S. 1974, *Ann. Rev. Astr. Ap.*, **12**, 331.
Minkowski, R., and Aller, L. H. 1956, *Ap. J.*, **114**, 93.
Osmer, P. S. 1976, *Ap. J.*, **203**, 352.
Osterbrock, D. E. 1974, *Astrophysics of Gaseous Nebulae* (San Francisco: Freeman), p. 66.
———. 1977, *Ap. J.*, **215**, 733.
Osterbrock, D. E., and Miller, J. S. 1975, *Ap. J.*, **197**, 535.
Peimbert, M. 1973, *Mém. Soc. Roy. Sci. Liège*, **5**, 307.
———. 1975, *Ann. Rev. Astr. Ap.*, **13**, 113.
Peimbert, M., and Torres-Peimbert, S. 1971, *Bols. Obs. Tonantzintla y Tacubaya*, **6**, 21.
Phillips, M. M., and Osterbrock, D. E. 1975, *Pub. A.S.P.*, **87**, 949.
Robinson, L. B., and Wampler, E. J. 1972, *Pub. A.S.P.*, **84**, 161.
———. 1973, in *Astronomical Observations with Television-Type Sensors*, ed. J. W. Glaspey and G. A. H. Walker (Vancouver: University of British Colombia), p. 69.
Stone, R. P. S. 1974, *Ap. J.*, **193**, 135.
———. 1977, *Ap. J.*, **218**, 767.
Webster, B. L. 1969, *M.N.R.A.S.*, **143**, 79.
Whitford, A. E. 1958, *A.J.*, **63**, 201.

HOLLAND C. FORD and GEORGE H. JACOBY: Department of Astronomy, University of California, 405 Hilgard Avenue, Los Angeles, CA 90024

DAVID C. JENNER: Department of Astronomy, University of Washington, Seattle, WA 98195